Title	A comparative study on the dielectric functions of isolated Si nanocrystals and densely-stacked Si nanocrystal layer embedded in SiO2 synthesized with Si ion implantation
Author(s)	Ding, Liang; Chen, Tupei; Liu, Yang; Liu, Yu Chan
Citation	Ding, L., Chen, T., Liu, Y., & Liu, Y. C. (2008). A comparative study on the dielectric functions of isolated Si nanocrystals and densely-stacked Si nanocrystal layer embedded in SiO2 synthesized with Si ion implantation. Silicon photonics III.
Date	2008
URL	http://hdl.handle.net/10220/6938
Rights	

A comparative study on the dielectric functions of isolated Si nanocrystals and densely-stacked Si nanocrystal layer embedded in SiO_2 synthesized with Si ion implantation

L. Ding*[a], T. P. Chen[a], Y. Liu[a], and Y. C. Liu[b]
[a]School of Electrical and Electronic Engineering, Nanyang Technological University, Singapore 639798; [b]Singapore Institute of Manufacturing Technology, Singapore 638075

ABSTRACT

Both isolated Si nanocrystals (*nc*-Si) dispersedly distributed in a SiO_2 matrix and densely stacked *nc*-Si layers embedded in SiO_2 have been synthesized with the ion implantation technique followed by high temperature annealing. The dielectric functions of the isolated *nc*-Si and densely-stacked nc-Si layer embedded in SiO_2 have been determined with spectroscopic ellipsometry (SE) in the photon energy range of 1.1-5 eV. The dielectric functions of these two different Si nanostructures were successfully extracted from the SE fitting based on a multi-layer fitting model that takes into account the distribution of *nc*-Si in SiO_2 and a five phase model (i.e., air/SiO_2 layer/densely-stacked *nc*-Si layer/SiO_2 layer/Si), respectively. The dielectric spectra of isolated *nc*-Si distributed in SiO_2 present a two-peak structure, while the dielectric spectra of densely-stacked *nc*-Si layer show a single broad peak, being similar to that of amorphous Si. The dielectric functions of these two Si nanostructures both show significant suppressions as compared with bulk crystalline Si. However, it has been observed that the densely stacked *nc*-Si layer exhibits a more significant suppression in the dielectric spectra than the isolated *nc*-Si dispersedly embedded in SiO_2. This is probably related to the two factors: (i) the *nc*-Si size (~3 nm) of the densely stacked *nc*-Si layer is smaller than that (~4.5 nm) of the isolated *nc*-Si embedded in SiO_2 matrix, and (ii) the densely stacked *nc*-Si layer has an amorphous phase.

Keywords: Si nanocrystals, implantation, dielectric function, ellipsometry

1. INTRODUCTION

There has been increasing research interest in Si nanostructures since the discovery of strong photoluminescence (PL) from porous Si.[1] Si nanocrystals (*nc*-Si) embedded in a dielectric matrix have been extensively studied as they provide the possibility for applications in Si-based optoelectronic devices, memory devices, and single electron devices with the advantage of being compatible with the mainstream complimentary metal-oxide-semiconductor (CMOS) technology in the semiconductor industry.[1-5] Various techniques have been employed to synthesize *nc*-Si, including chemical vapor deposition (CVD),[2,3] silicon ion implantation into SiO_2,[4-7] sputtering,[8,9] and pulse laser deposition (PLD).[10,11] Among all these techniques, silicon ion implantation into a SiO_2 matrix followed by high temperature annealing is considered as one of the most promising methods for producing chemically and electrically stable *nc*-Si. It also allows for an accurate control of the depth distribution of *nc*-Si within the SiO_2 film and yields a smaller size (<10 nm) and a narrow size distribution of the *nc*-Si. With this technique, both isolated *nc*-Si dispersedly distributed in a SiO_2 matrix[6,7] and densely stacked *nc*-Si layers embedded in SiO_2[12-15] can be synthesized depending on the implantation recipe.

The optical properties of continuous thin film of *nc*-Si synthesized by pulse laser pyrolysis of silane have been determined with spectroscopic ellipsometry.[16] However, there have been few studies that deal with the experimental determination of the optical properties of densely stacked *nc*-Si layer embedded in a dielectric matrix. The optical properties of the densely stacked *nc*-Si layer should be different from that of both isolated *nc*-Si and continuous film of *nc*-Si. In addition, a comparative study on the dielectric functions of dispersedly distributed *nc*-Si in SiO_2 and densely stacked *nc*-Si layer is needed for a comprehensive understanding of the optical properties of *nc*-Si synthesized by ion implantation. Dispersedly distributed Si nanocrystals can be formed in SiO_2 matrix with a high dose of Si ions implanted at a high or medium energy.[6,7] In practical applications, a high dose (typically in the range of ~10^{16}-~10^{17} cm^{-2}) Si ion implantation at a very-low energy (≤2 keV) into a thin SiO_2 film can form a densely stacked *nc*-Si layer embedded in the SiO_2 matrix.[12-15] In this work, the dielectric functions of dispersedly Si nanocrystals and densely stacked *nc*-Si layer embedded in SiO_2 have been determined with spectroscopic ellipsometry (SE).

*ding0008@ntu.edu.sg

Silicon Photonics III, edited by Joel A. Kubby, Graham T. Reed
Proc. of SPIE Vol. 6898, 68980I, (2008) · 0277-786X/08/$18 · doi: 10.1117/12.762600

2. EXPERIMENTS

The dispersedly distributed *nc*-Si embedded in a SiO_2 matrix was synthesized by Si+ implantation with a dose of 10^{17} atoms/cm^2 at the energy of 100 keV into a 550-nm-thick SiO_2 film thermally grown on a *p*-type Si substrate. A thermal annealing at 1000 °C for 30 min in nitrogen gas was carried out for the formation of Si nanocrystals dispersedly distributed in the SiO_2 film. The *nc*-Si distribution in the SiO_2 thin film can be determined from the secondary ion mass spectroscopy (SIMS) measurement. The SIMS intensity $I(x)$ due to the excess silicon in the Si^+-implanted region at a given depth (x) can be obtained by deducting the Si SIMS signal of the pure SiO_2 region from the measured total Si SIMS signal which is from both the excess Si and the SiO_2 at the depth. The amount of excess Si at depth x should be proportional to the intensity $I(x)$. The volume fraction of *nc*-Si at the depth should be proportional to the amount of the excess Si at the depth. Thus, the volume fraction $f(x)$ of the *nc*-Si embedded in SiO_2 at depth x can be expressed as

$$f(x) = \frac{QI(x)}{N\mathrm{si}\int_0^{d_{\max}} I(x)dx} \tag{1}$$

where Q is the dose of implanted Si ions in the unit of atoms/cm^2, $d_{\max}$ is the maximum depth in SiO_2 beyond which no excess Si can be detected, and N_{Si} is the Si density in the unit of atoms/cm^3. In this study, Q is equal to10^{17} atoms/cm^2 and N_{Si} is 5×10^{22} atoms/cm^3. Figure 1(a) shows the high resolution transmission electron microscopy (HRTEM) image of the *nc*-Si with an average diameter of ~4.5 nm dispersedly embedded in the SiO_2 matrix. Densely-stacked *nc*-Si layer were synthesized as follows. 30-nm SiO_2 thin films were thermally grown in dry oxygen at 950 ^{o}C on *p*-type (100) wafers. Si ions with a dose of 8×10^{16} cm^{-2} were then implanted into the SiO_2 thin films at the energy of 1 keV. Postimplantation thermal annealing was carried out in the N_2 ambient at 1000 ^{o}C for 30 min. A densely stacked *nc*-Si layer with the thickness of ~16 nm embedded in SiO_2 is observed from the cross-sectional transmission (TEM) image, as shown in Fig. 1(b). The mean size of *nc*-Si is ~3 nm as determined from full width at half-maximum (FWHM) of the Bragg peak in the X-ray diffraction (XRD) measurements. Spectroscopic ellipsometry (SE) measurements were carried out in the wavelength range of 250-1100 nm with a step of 5 nm at the incident angle of 75^o to determine the dielectric functions of the densely stacked *nc*-Si layer.

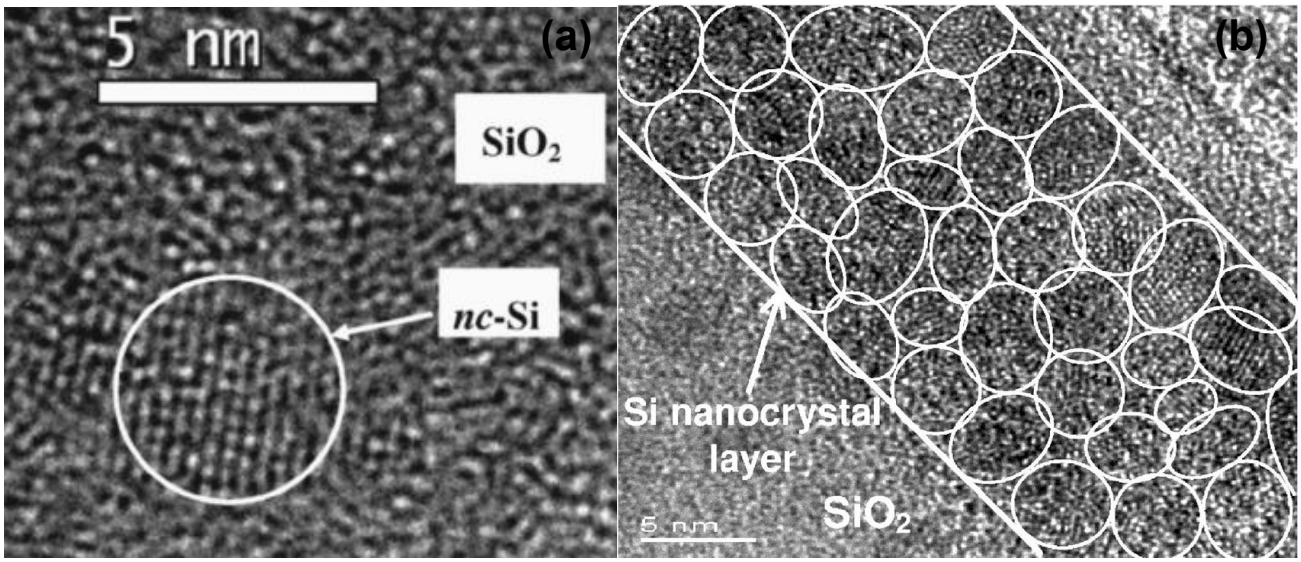

Fig. 1. (a) TEM image of dispersedly distributed nc-Si embedded in SiO_2; (b) TEM image of the densely-stacked nc-Si layer embedded in SiO_2.

3. METHODOLOGY

The implanted Si distributes from the surface to the depth of ~250 nm, and the subsequent annealing does not change the profile significantly because of the extremely low diffusion coefficient of Si in SiO_2 films. There is almost no *nc*-Si beyond the depth of 250 nm in the SiO_2 film. In order to extract the dielectric functions of *nc*-Si embedded in SiO_2, the multilayer optical model shown in Fig. 2(a) was used to analyze the SE data. As can be seen in Fig. 2(a), the layer containing *nc*-Si, whose thickness $d1$ is 250 nm, is divided into 25 sublayers with equal thickness d_0=10 nm. Each

sublayer can be optically schematized as an effective medium represented by the Maxwell-Garnett effective medium approximation (EMA). The Maxwell-Garnett EMA is characterized by the volume fraction of *nc*-Si which can be obtained from the SIMS measurement, the known dielectric functions of SiO_2, and the *nc*-Si dielectric functions that are to be determined. Therefore, the Maxwell-Garnett EMA can be used to extract the *nc*-Si dielectric functions from the SE spectral fitting. For the spectral fitting an optical dispersion model for the *nc*-Si is required. We have found that the four-term FB model[17] is the suitable one that can yield a successful fitting. As such, the Maxwell-Garnett EMA based on the four-term FB model is used in the SE spectral fitting. In the spectral fitting, the optimization is carried out by freely varying the 14 parameters,[17] which include the parameters A_i ,B_i ,C_i (i=1, 2, 3, and 4) for the four terms, the refractive index (n) when photon energy $E \rightarrow \infty$, and the band gap E_g to minimize the mean-square error (MSE) (Ref. 18).

In the initial SE analysis for the samples with densely-stacked *nc*-Si layer embedded in SiO_2, we also tried to employ the multilayer model to fit the SE spectra, but no reasonable fittings could be achieved. This indicates that the multi-layer model is inadequate for the densely-stacked *nc*-Si layer synthesized with a high-dose (5×10^{16} cm^{-2}) at very-low energy (1 keV). Therefore, a new model is required for the present study. In this study, as a densely stacked *nc*-Si layer is formed in the SiO_2 thin film, this *nc*-Si layer should be treated as one phase in the SE analysis. Therefore, in the SE analysis, the material system of the present study can be described by the five-phase model (i.e., air/SiO_2 layer/densely stacked *nc*-Si layer/SiO_2 layer/ Si substrate), as shown in Fig. 2 (b). In the fitting, the ellipsometric angles (Ψ and Δ) which are functions of both the film thickness and the optical constants of all the layers were fitted at each wavelength, thus no optical dispersion equation was required with the five-phase model.

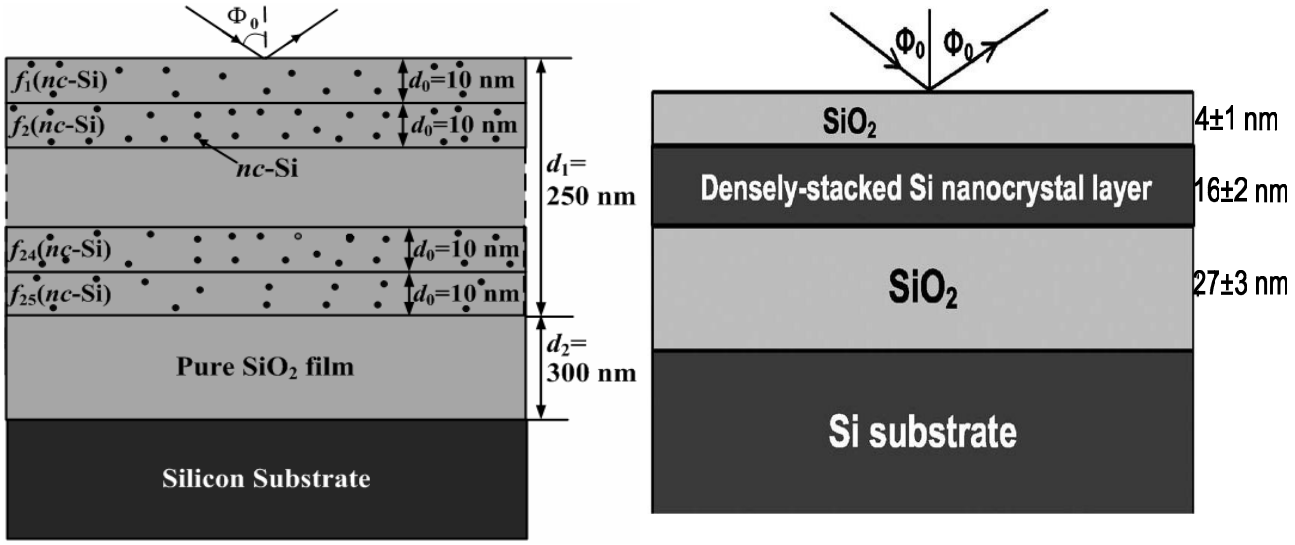

Fig. 2. (a) Multilayer model in the extraction of dielectric functions of dispersedly distributed nc-Si embedded in SiO_2; (b) Five-phase model used in the SE analysis for the determination of densely-stacked nc-Si layer embedded in SiO_2.

4. RESULTS AND DISCUSSIONS

Based on the methods mentioned above, excellent spectral SE fitting were achieved for both the dispersedly distributed *nc*-Si and densely-stacked *nc*-Si layer. Figure 3 shows the best spectral fittings for the dispersedly distributed *nc*-Si and densely-stacked *nc*-Si layer embedded in SiO_2 films. As can be seen in this figure, all the complicated spectral features of both Ψ and Δ can be fitted excellently, indicating that the models shown in Fig. 2 are effective. Figure 3 shows the dielectric functions of the dispersedly distributed *nc*-Si and densely-stacked *nc*-Si layer obtained from the fitting shown in Fig. 2(b). For comparison, the dielectric functions of other Si materials including the continuous *nc*-Si thin film deposited by pulsed laser pyrolysis of silane (Ref. 16), amorphous Si (Ref. 19) and bulk crystalline Si (Ref. 20) are also included in Fig. 3. As can be seen in Figs. 4, the overall spectral features of dielectric functions of *nc*-Si are similar to that of bulk crystalline Si. However, the *nc*-Si shows a significant reduction in the optical constants and dielectric function as compared with bulk crystalline Si. It has been well established that reduction of the static dielectric constant becomes significant as the size of the quantum confined physical systems, such as quantum dots and wires, approaches the nanometric range.[21,22] However, the origin of the reduction in the static dielectric constant with the size is still not fully understood. It is often attributed to the opening of the gap, which should lower the polarizability, but it is also

shown that the reduction is due to the breaking of polarizable bonds at the surface and is not due to the opening of the band gap induced by the confinement.[23] As can be seen in the figure, the dielectric spectra of the densely-stacked silicon nanocrystal layer are similar to that of amorphous Si but different from those of both bulk crystalline Si and the isolated *nc*-Si. For the imaginary part of dielectric functions, the densely-stacked silicon nanocrystal layer and amorphous Si show a single broadened peak; in contrast, bulk crystalline Si and the isolated *nc*-Si exhibit a two-peak structure. The peak structures in the spectra of the imaginary part of dielectric functions are believed to originate from singularities in the joint density of states (DOS). Essentially, the DOS in the amorphous state is a broadened version of crystalline state, which leads to a single broad peak in the dielectric spectra of amorphous semiconductors. Therefore, the single broadened peak observed for the densely-stacked silicon nanocrystal layer may suggest that the nanocrystal layer is in an amorphous state to certain extent. On the other hand, the nanocrystal layer also shows significant dielectric suppressions (i.e., reductions in the dielectric functions) as compared with bulk crystalline silicon and amorphous silicon, which is believed to be related to the size effect of the nanocrystals.[6,7] Furthermore, it is observed that the dielectric functions of the densely-stacked *nc*-Si layer are suppressed much more than those of isolated *nc*-Si embedded in SiO_2. This are mostly related to: (i) the smaller size of nanocrystals (~3 nm) than that of isolated *nc*-Si, and (ii) the remaining amorphous phase of Si nanoclusters for the sample in this study. Therefore, we propose that the suppression of the dielectric spectra of the densely-stacked Si nanocrystal layer originates from both the quantum confinement effect and the remaining amorphous phase of the *nc*-Si layer, which also contributes to the single-peak structure of the dielectric spectra.

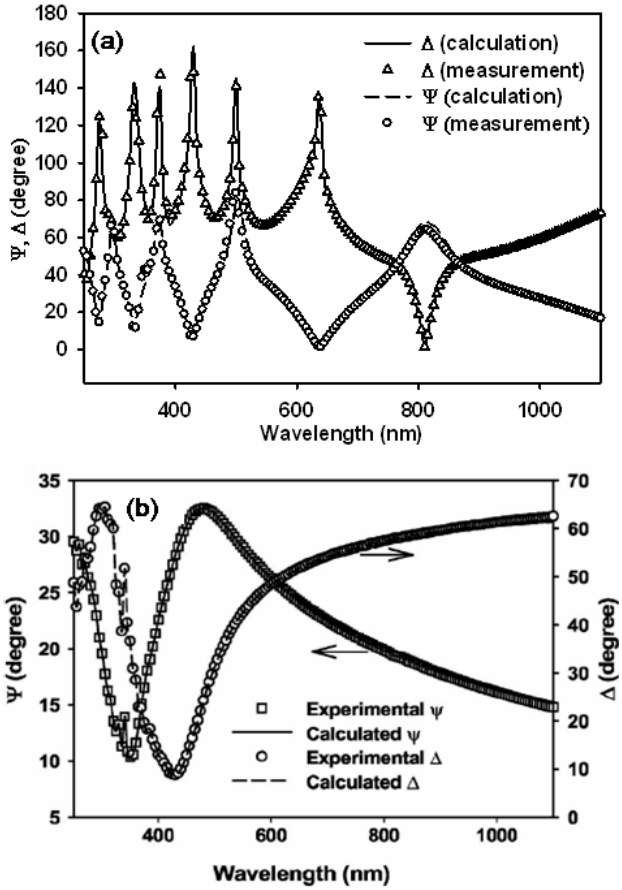

Fig. 3. (a) Best spectral fitting for the sample with dispersedly distributed nc-Si in SiO_2; (b) Best spectra fitting for the sample with densely-stacked nc-Si layer embedded in SiO_2.

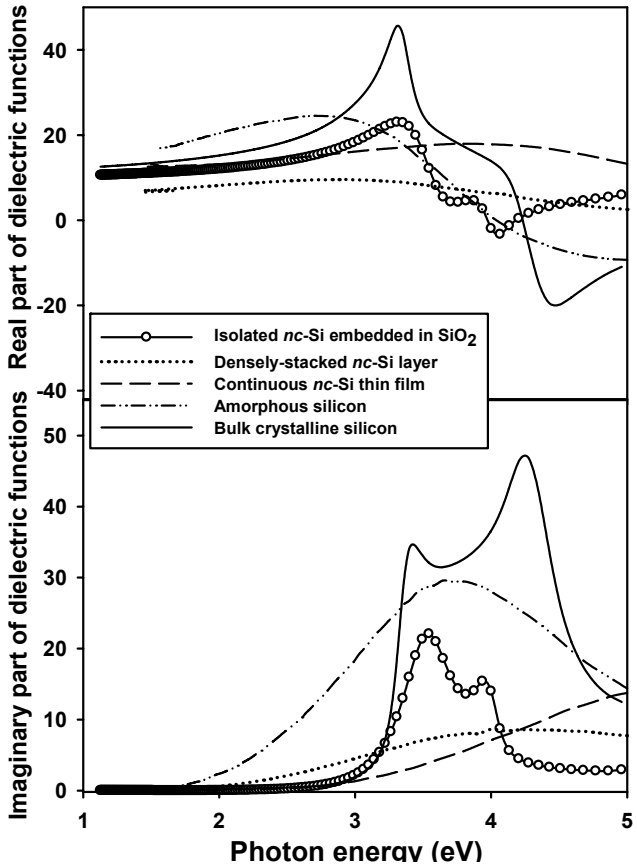

Fig. 4. (a) Real and imaginary parts of the complex dielectric functions of isolated *nc*-Si dispersedly distributed in a SiO_2 matrix, the densely-stacked Si nanocrystal layer. For comparison, the dielectric functions of the continuous *nc*-Si thin film (Ref. 14), amorphous Si (Ref. 16) and bulk crystalline Si (Ref. 17) are also included for comparison.

5. SUMMARY

In summary, isolated Si nanocrystals (*nc*-Si) dispersedly distributed in a SiO_2 matrix and densely stacked *nc*-Si layers embedded in SiO_2 have been synthesized with Si ion implantation and subsequent annealing. Dielectric functions of the two different *nc*-Si structures have been obtained in the photon energy range of 1.1-5.0 eV using SE analysis. The optical properties of the *nc*-Si dispersedly distributed in SiO_2 are found to be well described by the four-term Forouhi-Bloomer model. The dielectric spectra of the *nc*-Si dispersedly distributed in SiO_2 are similar to that of the bulk crystalline Si, although it shows a significant reduction as compared with bulk crystalline Si. The dielectric functions of the densely-stacked *nc*-Si layer embedded in SiO_2 synthesized by low-energy Si^+ implantation are suppressed much more than that of *nc*-Si dispersedly distributed embedded in SiO_2 formed by high-energy Si^+ implantation. It could be due to both the quantum confinement effect and the remaining amorphous phase of the densely-stacked *nc*-Si layer. The partially amorphous phase of the densely-stacked *nc*-Si layer also makes contributions to the single-peak structure of the dielectric spectra.

ACKNOWLEDGEMENT

This work has been financially supported by the Ministry of Education, Singapore, under project ARC No. 1/04 and the Singapore Millennium Foundation.

REFERENCES

[1] L. T. Canham, "Silicon quantum wire arrays fabricated by electrochemical and chemical dissolution of wafers," Appl. Phys. Lett. **57(10)**, 1046-1048 (1990).

[2] S. Tiwari, F. Rana, H. Hanafi, A. Hartstein, E. F. Crabbé, and K. Chan, "A silicon nanocrystals based memory," Appl. Phys. Lett. **68(10)**, 1377-1379 (1996).

[3] D. N. Kouvatsos, V. Ioannou-Sougleridis, and A. G. Nassiopoulou, "Charging effects in silicon nanocrystals within SiO_2 layers, fabricated by chemical vapor deposition, oxidation, and annealing," Appl. Phys. Lett. **82(3)**, 397-399 (2003).

[4] S. H. Choi and R. G. Elliman, "Reversible charging effects in SiO_2 films containing Si nanocrystals," Appl. Phys. Lett. **75(7)**, 968-970 (1999).

[5] L. Pavesi, L. Dal Negro, C. Mazzoleni, G. Franzo, and F. Priolo, "Optical gain in silicon nanocrystals," Nature (London) **408**, 440-444 (2000).

[6] T. P. Chen, Y. Liu, M. S. Tse, O. K. Tan, P. F. Ho, K. Y. Liu, D. Gui, and A. L. K. Tan, "Dielectric functions of Si nanocrystals embedded in a SiO_2 matrix," Phys. Rev. B **68(15)**, 153301 (2003).

[7] L. Ding, T. P. Chen, Y. Liu, C. Y. Ng, and S. Fung, Phys. Rev. B, "Optical properties of silicon nanocrystals embedded in a SiO_2 matrix," **72(10)**,125419 (2005).

[8] S. Furukawa and T. Miyasato, "Three-dimensional quantum well effects in ultra fine silicon particles," Jpn. J. Appl. Phys. Part 2, **27(11)**, L2207-L2209 (1988).

[9] Q. Zhang, S. C. Bayliss, and R. A. Hutt, "Blue photoluminescence and local structure of Si nanostructures embedded in SiO_2 matrices," Appl. Phys. Lett. **66(15)**, 1977-1979 (1995).

[10] T. Yoshida, S. Takeyama, Y. Yamada, and K. Mutoh, "Nanometer-sized silicon crystallites prepared by excimer laser ablation in constant pressure inert gas," Appl. Phys. Lett. **68(13)**, 1772-1774 (1996).

[11] X. Y. Chen, Y. F. Lu, Y. H. Wu, B. J. Cho, D. M. H. Liu, Y. Dai, and W. D. Song, "Mechanisms of photoluminescence from silicon nanocrystals formed by pulsed –laser deposition in argon and oxygen ambient," J. Appl. Phys. **93(10)**, 6311-6319 (2003).

[12] M. Carrada, N. Cherkashin, C. Bonafos, G. Benassayag, D. Chassaing, P. Normand, D. Tsoukalas, V. Soncini, and A. Claverie, "Effect of ion energy and dose on the positioning of 2D-arrays of Si nanocrystals ion beam synthesized in thin SiO_2 layers," Mater. Sci. Eng. B **101(2)**, 204-207 (2003).

[13] P. Normand, K. Beltsios, E. Kapetanakis, D. Tsoukalas, T. Travlos, J. Stoemenos, J. Van Den Berg, S. Zhang, C. Vieu, H. Launois, J. Gautier, F. Jourdan, and L. Palun, "Formation of 2-D arrays of semiconductor nanocrystals or semiconductor-rich nanolayers by very low-energy Si or Ge ion implantation in silicon oxide films," Nucl. Instrum. Methods Phys. Res. B **178(1-4)**, 74-77 (2001).

[14] C. Bonafos, M. Carrada, N. Cherkashin, H. Coffin, D. Chassaing, G. Benassayag, A. Claverie, T. Müller, K. H. Heinig, M. Perego, M. Fanciulli, P. Dimitrakis, and P. Normand, "Manipulation of two-dimensional arrays of Si nanocrystals embedded in thin SiO_2 layers by low energy ion implantation," J. Appl. Phys. **95(10)**, 5696-5702 (2004).

[15] C. Y. Ng, T. P. Chen, L. Ding, and S. Fung, "Memory characteristics of MOSFETs with densely-stacked silicon nanocrystal layers in the gate oxide synthesized by low-energy ion beam," IEEE Electron Device Lett. **27(4)**, 231-233 (2006).
[16] D. Amans, S. Callard, A. Gagnaire, J. Joseph, G. Ledoux, and F. Huisken, "Ellipsometric study of silicon nanocrystal optical constants," J. Appl. Phys. **93(7)**, 4173-4179 (2003).
[17] A. R. Forouhi and I. Bloomer, "Optical properties of crystalline semiconductors and dielectrics," Phys. Rev. B **38(3)**, 1865-1874 (1988).
[18] R. M. A. Azzam and N. M. Basharra, *Ellipsometry and Polarized Light*, North-Holland, Amsterdam, 1977.
[19] D. E. Aspnes, A. A. Studna, and E. Kinsbron, "Dielectric properties of heavily doped crystalline and amorphous silicon from 1.5 to 6.0 eV," Phys. Rev. B **29(2)**, 768-780 (1984).
[20] D. E. Aspnes and A. A. Studna, Phys. Rev. B "Dielectric functions and optical parameters of Si, Ge, GaP, GaAs, GaSb, InP, InAs, and InSb from 1.5 to 6.0 eV," **27(2)**, 985-1009 (1983).
[21] R. Tsu, D. Babic, and L. Ioriatti, "Simple model for the dielectric constant of nanoscale silicon particle," Jr., J. Appl. Phys. **82(3)**, 1327-1329 (1997).
[22] L.-W. Wang and Alex Zunger, "Pseudopotential calculations of nanoscale CdSe quantum dots," Phys. Rev. B **53(15)**, 9579-9582 (1996).
[23] C. Delerue, M. Lannoo, and G. Allan, "Concept of dielectric constant for nanosized systems," Phys. Rev. B **68(11)**, 115411 (2003).